(This is a preprint of an article to appear in the 1997 Ultrasonics Symposium Proceedings)

Pseudospectral Methods for Large-Scale Bioacoustic Models

G. Wojcik, B. Fornberg†, R. Waag‡, L. Carcione, J. Mould, L. Nikodym, T. Driscoll†

Weidlinger Associates, Inc., 4410 El Camino Real, Suite 110, Los Altos, CA 94022
†Department of Applied Mathematics, University of Colorado, Boulder, CO 80309
‡Department of Electrical Engineering, University of Rochester, Rochester, NY 14627

Abstract — Large-scale simulations of ultrasonic waves in heterogeneous tissue models are useful in biomedical R&D for imaging and therapeutics. The scale of bioacoustic models is hundreds of wavelengths. Typical 2D wave solvers are not practical at this scale, and 3D is out of the question, because of numerical errors and/or computer limits. To achieve much higher performance we use the periodic pseudospectral (PS) method, where spatial derivatives are calculated from FFTs over Cartesian grids. With a 4th order explicit time integrator, the PS method yields the necessary accuracy and efficiency. However, the domain must be periodic. We show how to circumvent this intrinsic limitation with Berenger's perfectly matched layer (PML) on the boundaries. High accuracy, computational efficiency, and parallelism are demonstrated and a large-scale bioacoustic model is calculated. Generalizations of the method are described, including attenuation and nonlinearity.

Introduction

Bioacoustic simulations are numerical calculations of scalar waves through heterogeneous, lossy tissue models. For medical imaging the needs are accurate, large-scale, broadband solutions of wavefront aberrations, back-scattering by tissue structure ($c \approx 1550 \pm 100$ m/s), e.g., see [1], and perhaps weak shock effects. Therapeutic applications require, in addition, narrowband solutions of focused beams including nonlinearities due to high intensities and, perhaps, scattering by induced structure, like bubbles, e.g., [2]. The principal difficulty with bioacoustic modeling in real tissue cross-sections is the long propagation distance. For example, over a 10 cm round-trip or direct travel path, 5 MHz waves propagate 333 wavelengths. At these ranges, typical finite element (FE) or finite difference (FD) algorithms distort signals unacceptably. The reason is that production wave solvers use local, low order space and time derivative approximations to achieve modeling versatility and computational efficiency rather than ultimate numerical accuracy.

Long range wave distortion is caused by artificial spatial and temporal sampling that make numerical phase velocity and attenuation depend on direction and frequency. For example, Fig. 1 illustrates 1D wave solutions that are 2nd order accurate in space (FE or FD) and time (central difference). A wavelet is applied at one end of a long model and propagated past a point 300 wavelengths away. Results are cross-plotted in Fig. 1 for a practical spatial sampling of 20 elements/wave at the wavelet's center frequency of 2.5 MHz with timestep $\Delta t = 0.99\Delta x/c$ and $\Delta t = 0.8\Delta x/c$. Note that $\Delta x/c$ is the Courant stability number for the grid, Δx is the spatial interval, and c is continuum wavespeed. We will often refer to the so-called Courant stability factor τ instead of timestep, where $\Delta t = \tau \Delta x/c$. The smaller stability factor, $\tau = 0.8$, is a typical value for heterogeneous tissue, but spatial and temporal errors virtually destroy the wavelet at this range. Fourier transforms of these waveforms show identical amplitude spectra, so pulse distortion is due to phase errors, i.e., dispersion, not numerical damping.

This and similar numerical wave errors are the bane of analysts attempting full-scale bioacoustic simulations. Conventional (low order) FE and FD algorithms can be tuned for accuracy, but only to a limited degree. The k-space [3,4] and pseudospectral [5,6] methods offer attractive alternatives by virtue of very accurate Fourier interpolation in space, i.e., FFTs are used to evaluate spatial derivatives on a uniform Cartesian mesh. In this paper we utilize the mathematically simpler pseudospectral (PS) method, motivated by recent work on the k-space method [7]. In conjunction with an appropriate time-integration scheme, the PS method can yield accurate solutions, i.e., virtually no distortion. High spatial accuracy permits relatively coarse, inexpensive grids limited by density and

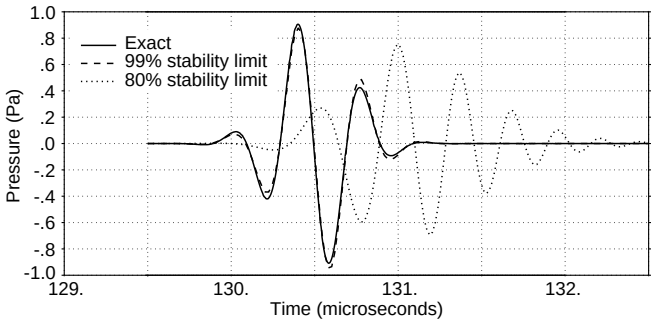

Fig. 1. Comparison of wavelet time histories after propagating 300 wavelengths in a 1D, 2nd order accurate grid (FE or FD).

stiffness variations. There is no need to transform the inhomogeneous wave equation, only the solution vector. Note that pressure-density (constitutive) nonlinearity is readily included since the differential equation is not transformed. The price to be paid for high accuracy is a periodic space domain by virtue of the Fourier basis.

Periodicity has been the principal limitation of PS methods for production wave solvers. Conventional radiation boundary conditions for low order FD and FE methods are not appropriate for PS boundary conditions because of the periodic Fourier basis. Efforts to circumvent periodicity range from simple padding to boundary "tapers," e.g., see [8]. As alluded to in [8], a better solution would be an absorbing, reflectionless, border or layer that makes the solution periodically zero. Berenger's invention [9] of the perfectly matched layer (PML) may finally yield such a solution. To this end we demonstrate Berenger's PML on a PS solver for the inhomogeneous acoustic wave equation. This is a new combination of fundamental techniques and its advantages are demonstrated. In particular, we examine distortion, validate PS results against an exact scattering solution, quantify model performance and size advantages, describe symmetric multiprocessor (SMP) computing, and discuss necessary generalizations.

Acoustic Wave Equations

To simulate ultrasound in tissue models we solve the governing partial differential equations (PDEs), which follow from the momentum and constitutive equations,

$$\rho \frac{\partial^2 u}{\partial t^2} = -\nabla p \quad , \quad p = -K \nabla \cdot u \tag{1}$$

where $u=(u_x,u_y,u_z)^T$ is the displacement vector, p is pressure, ρ is density, $K=\rho c^2$ is bulk modulus, and c is wavespeed. Coefficients ρ, K, and c are functions of space. Eliminating p in (1) yields the wave equation on u, however, spatial derivatives of ρ and c appear through $\nabla K=c^2\nabla\rho+2\rho c\nabla c$. Alternately, differentiating the constitutive equation with respect to time yields the first order system on velocity vector $v=(v_x,v_y,v_z)^T$ and pressure rate,

$$\frac{\partial v}{\partial t} = -\frac{1}{\rho}\nabla p \quad , \quad \frac{\partial p}{\partial t} = -K \nabla \cdot v \tag{2}$$

which does not involve explicit derivatives of coefficients.

The discrete, 2D form of (2) is written by restricting velocity and pressure to the N points of a $N=N_x \times N_y$ Cartesian grid. Defining N-vectors on velocities V_x, V_y and pressure P and ordering elements for computational efficiency, the system of discrete equations is

$$\frac{\partial W}{\partial t} = f(W) \quad , \quad W \equiv \left(V_x \, , V_y \, , P\right)^T$$
$$f(W) = \left(-\frac{1}{\rho}\frac{\partial P}{\partial x} \, , -\frac{1}{\rho}\frac{\partial P}{\partial y} \, , -K\left(\frac{\partial V_x}{\partial x} + \frac{\partial V_y}{\partial y}\right)\right)^T \tag{3}$$

where W is the work vector of length 3N and the T superscript denotes the transpose. This is reduced to a system of ordinary differential equations (ODEs) by evaluating the spatial derivatives.

Pseudospectral Method

The periodic pseudospectral method uses discrete Fourier transforms to evaluate spatial derivatives of functions defined on a uniform Cartesian grid. On this basis, time-dependent PDEs are reduced to ODEs, which are integrated forward in time using either explicit or implicit methods. As with FD and FE methods, the PS gridpoints must be dense enough to resolve spatial details of the PDE coefficients over the domain. However, unlike uniform difference stencils or element meshes, the PS method is global and yields a very high order spatial derivative approximation, equal to the number of grid points in each direction, e.g., N_x and N_y. Fornberg [6] has shown formal equivalence between the PS method and N_xth and N_yth order finite difference stencils. This is the reason for its high spatial accuracy. The practical disadvantage is spatial periodicity, which exhibits itself as "wraparound" of the field, i.e., waves exit one side of the grid and enter from the opposite side.

Recall that if $\hat{u}(k)$ is the Fourier transform of $u(x)$ with spatial frequency (transform parameter) k, then the derivative of $u(x)$ is the inverse Fourier transform of $jk\hat{u}(k)$, where $j=\sqrt{-1}$. Therefore, calculation of the first derivative on a gridline of N points by the periodic PS method is done in three steps, e.g., from [6]: do a complex FFT on gridpoint data values, giving

$\hat{u}_0 \; \hat{u}_1 \; \hat{u}_2 \; \cdots \; \hat{u}_{N/2-1} \; \hat{u}_{N/2} \; \hat{u}_{N/2+1} \; \cdots \; \hat{u}_{N/2-2} \; \hat{u}_{N-1}$;
multiply these output elements by discrete spatial frequencies
$0 \; \pi j \; 2\pi j \; \cdots \; (N/2-1)\pi j \; 0 \; -(N/2-1)\pi j \; \cdots \; -2\pi j \; -\pi j$;
and perform a complex inverse FFT on the result. This yields the PS derivative approximation at the gridpoints. Since the procedure gives a real derivative from real data and the complex FFT is linear, we can initialize the real and imaginary parts of the FFT input with two independent real data sets and recover derivatives of each in the real and imaginary outputs.

Therefore, the solution algorithm for hyperbolic system (3) over one timestep is: load new values of V_x, V_y, P into W; calculate spatial derivatives of V_x, V_y, P on gridlines; evaluate f(W) and integrate the resulting system one timestep. This sequence is repeated as many times as necessary to capture the wave phenomena of interest. Note that incident waves are defined as initial conditions, typically pressure and velocity, over the entire grid. An example of scattering by a cylinder is shown in Fig. 2, using the above 2D algorithm with a 4th order Runge-Kutta integrator. Snapshots at early and later times illustrate wraparound due to periodicity of the PS method.

Integration and Accuracy

Applying the PS method to the hyperbolic system of PDEs in (3) yields the system of ODEs, dW/dt = f(W),

to be integrated in time. There are many effective integrators available, both implicit and explicit. Typically, implicit schemes are unconditionally stable, i.e., permit any Δt, but require solutions of matrix equations that are prohibitively expensive for large-scale problems. Explicit schemes are a much better choice for wave propagation because, despite their conditional stability, i.e., $\Delta t \leq \Delta t_{max}$, Δt is usually dictated by accuracy rather than stability requirements, and no matrix manipulation is necessary. Common explicit schemes are central differences (2nd order), Runge-Kutta (typically 4th order), and a host of multi-step methods.

The wave propagation example in Fig. 1 used a balanced algorithm, i.e., 2nd order in both space and time. This is computationally efficient because it produces the same order of temporal and spatial errors. Note that balance is the reason for so-called superconvergence at τ =0.99 in Fig. 1, due to cancellation of the same order time and space errors. This is impractical in heterogeneous media, however. Since spatial accuracy for the PS method is very high, in principle, the time integrator's order should be as high as possible. To explore the options we apply central difference (2nd order), Runge-Kutta (4th order), Adams-Bashforth (4th order), and various predictor-corrector schemes to the 1D problem used for Fig. 1. Time histories are cross-plotted in Fig. 3. The grid has 10 nodes per wavelength at the wavelet's center frequency.

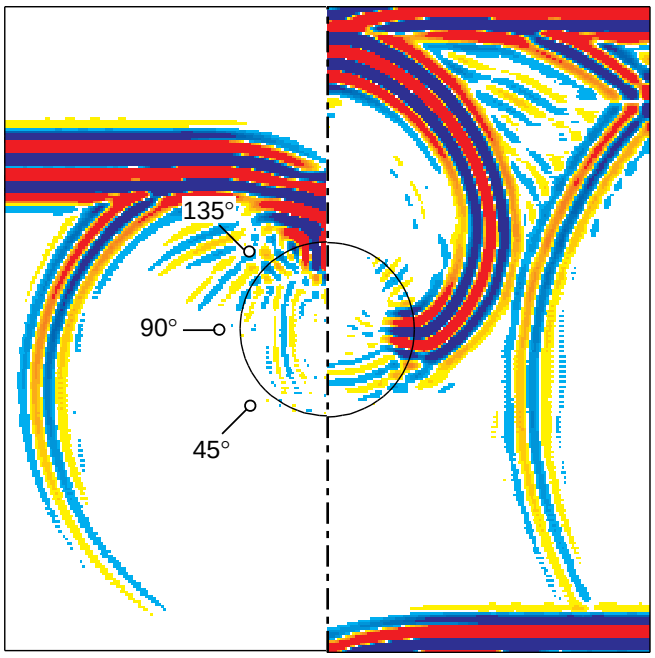

Fig. 2. Snapshots before (left) and after (right) wraparound of plane wave scattering by a slower cylinder in water, using the 2D PS/Runge-Kutta method.

The (2nd order) central difference or leapfrog scheme is by far the simplest and cheapest. It requires only one evaluation of the ODE's right hand side, f(W), at each timestep. However, numerical experiments indicate that without special tuning, the Courant stability factor for PS/leapfrog is relatively low, $\tau < 0.3$. Fourier transforms of long range waveforms using τ=0.125 show that the amplitude spectrum is preserved, hence, distortion is by dispersion only. Note that for PS/leapfrog, dispersion is anomalous (high frequencies travel faster) . In their generalization of the k-space method [4], Liu and Waag [7] show that in weakly inhomogeneous models, the stable timestep can be increased to 60% and more by tuning the difference operator.

In practice, the easiest higher order explicit scheme is 4th order Runge-Kutta (R-K). It requires four function evaluations at each timestep, hence, costs four times more than leapfrog with the same timestep and uses more memory. It is stable at τ=0.5. Fourier transforms show that the PS/R-K errors are due to light damping of higher frequencies. Accuracy is much better than for leapfrog with the same amount of computation (function evaluations), i.e., at 1/4 the R-K timestep. One drawback of R-K is that three of the function evaluations are "within" the timestep interval and cannot be reused.

Multi-step methods permit reuse of function evaluations and provide an effective means to trade memory for computations. A popular 4th order multi-step scheme is Adams-Bashforth, which advances the solution from derivatives at the three previous (stored) and the current timesteps. Hence, only one function evaluation is necessary per timestep. The PS/A-B scheme is found to give the highest accuracy at long ranges, although the stable timestep is relatively low, about that of leapfrog. Hence, A-B cost is comparable to that of R-K but it yields significantly higher accuracy.

Predictor-corrector schemes use an explicit multi-step operator to provide values for an implicit multi-step operator. Combining Adams-Bashforth (explicit) with Adams-Moulton (implicit) yields a popular 4th order predictor-corrector that requires two function evaluations per timestep.

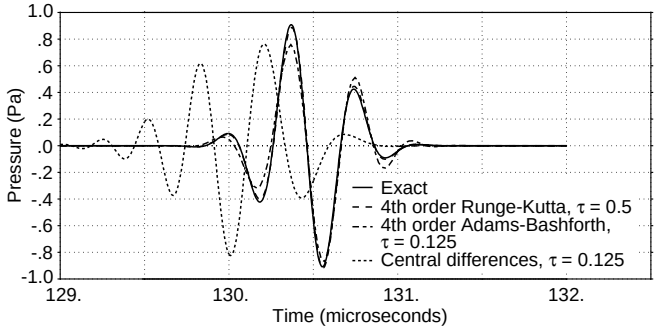

Fig. 3. Comparison of wavelet time histories after 300 wavelengths in a PS grid integrated in time by leapfrog, Runge-Kutta, and Adams-Bashforth.

At the ranges required for bioacoustic simulations, this and other predictor-corrector schemes damp the solution unacceptably, caused by the implicit corrector. In general, implicit schemes damp waves, which is responsible for their unconditional stability but makes them unsuitable for accurate, long range propagation.

Berenger's Perfectly Matched Layer (PML)

Berenger [9] showed how to construct the wave equation for a nonphysical medium that is highly attenuative yet nonreflective at any angle of incidence. The objective was efficient radiation boundary conditions for FD grids, in the context of wave equations for TE and TM electromagnetic field polarizations. Therefore, his approach is directly applicable to the acoustic wave equation (but not to the vector elasticity equations). The acoustic version for 2nd order, finite difference, time-domain solvers is described by Yuan, et. al [10], who demonstrated that waves incident from the grid's interior on an eight-node boundary layer are rapidly absorbed, with spurious reflections reduced by 80 dB.

In particular, [10] shows that to write the acoustic analog to Berenger's electromagnetic PML, it is only necessary to split pressure p into $p=p_x+p_y+p_z$ and introduce anisotropic attenuation coefficients α_x, α_y, α_z. The 2D acoustic PML equations then become

$$\frac{\partial v_x}{\partial t} = -\frac{1}{\rho}\frac{\partial p}{\partial x} - K\alpha_x v_x \quad , \quad \frac{\partial v_y}{\partial t} = -\frac{1}{\rho}\frac{\partial p}{\partial y} - K\alpha_y v_y$$
$$\frac{\partial p_x}{\partial t} = -K\frac{\partial v_x}{\partial x} - K\alpha_x p_x \quad , \quad \frac{\partial p_y}{\partial t} = -K\frac{\partial v_y}{\partial y} - K\alpha_y p_y \qquad (4)$$

These can replace acoustic equations (2) everywhere, with $\alpha_x=\alpha_y=0$ in the interior and nonzero near the boundaries. For computational efficiency, however, (4) should only be applied in a layer near the boundary, say over eight grid points. Smoothly increasing attenuation through this layer turns out to be optimal in order to absorb small reflections introduced by discretization of the continuum PML equations.

Therefore, we apply the PS method to (4) by a simple generalization of (3). Eight nodes near the boundary are "activated" i.e., have nonzero α. The problem remains periodic but "periodically small" at the boundaries, i.e. field values are driven towards zero there by the PML. Wraparound causes signals to do a double pass through the absorber, e.g., as an outgoing wave enters the PML on one side it is attenuated and any signal reaching the boundary enters the PML at the opposite boundary where it is further attenuated.

Validation

To validate the PS method with Berenger's PML we consider scattering of a plane wave in water by a soft acoustic cylinder. Radius of the cylinder is 3 mm and its wavespeed is 1200 m/s, compared to 1500 m/s in water. A 256x256 PS-PML grid with nodal spacing of 58 micrometers is used in order to include initial wave conditions and capture spatial frequency content. The stairstep approximation of the cylinder interface is fairly refined. The PS solution is compared to a truncated series solution (analytical) at 45°, 90°, and 135° from the leading edge, on a 4 mm radius circle. These points are indicated in Fig. 2, which was calculated without the PML. Applying the PML and cross-plotting analytical and numerical results yields the excellent agreement in Fig. 4. Discernible phase errors are due to output location mismatch, i.e., grid points closest to the specified output coordinate. In general, the PML condition works very well and noise for this implementation is $O(10^{-5})$ of the input (-100 dB).

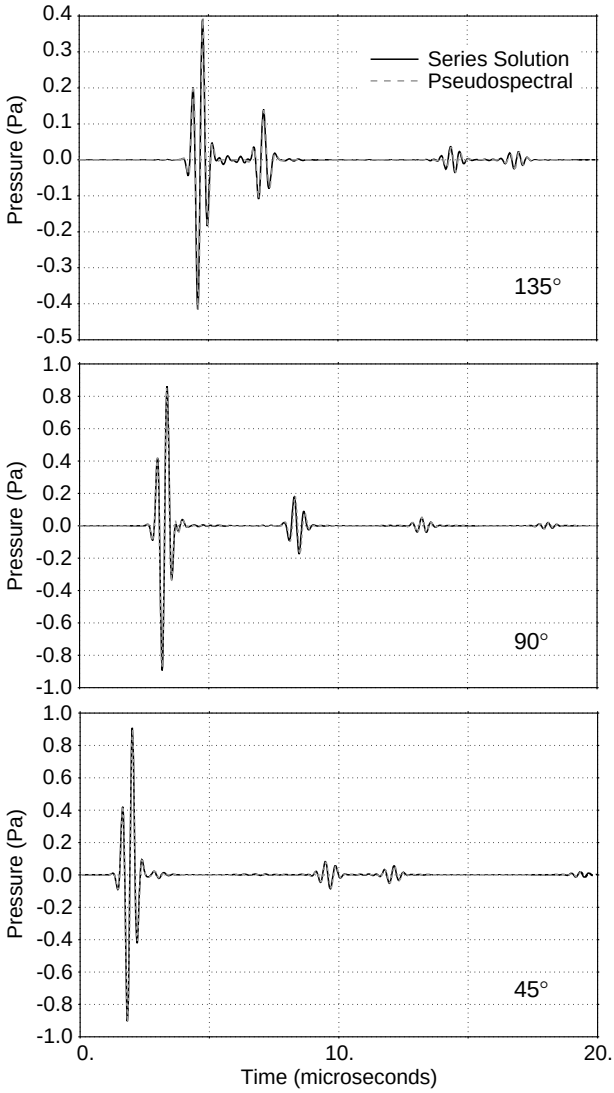

Fig. 4. Validation of the PS method and PML against a truncated series solution at the output points indicated in Fig. 2.

Initialization

There are no boundaries in the PS space domain, only periodicity. Therefore, initial conditions, i.e., at a single time over all space, are commonly used for wave input to the problem. Two initial conditions, e.g., pressure and velocity, start unidirectional wave motion. A single initial condition yields waves traveling in "opposite" directions on the two characteristic surfaces in x,y,t space. Alternatively, we can consider introducing an internal boundary condition, i.e., initializing the wave field on single space line for all time. Prescribing pressure and velocity on the space line yields a unidirectional wave, while prescribing pressure or velocity yields waves traveling in opposite directions. The unwanted wave is absorbed by the PML. The 1D and 2D examples shown above were driven by initial conditions over the grid. However, we have demonstrated the same results with an internal boundary condition. For example, this permits the validation problem, Fig. 4, to be calculated on a 64x64 grid with no discernible difference in wave arrivals.

Parallelization

The relevant scales for large bioacoustic problems are, say, 0.3 mm waves (5 MHz) in a 10x10(x10) cm tissue model. 4 nodes/wave in a homogeneous model suffice for the PS method, which requires 333x333(x333) wavelengths or $\approx 1.8 \times 10^6$ nodes in 2D ($\approx 2.4 \times 10^9$ in 3D). To capture details of tissue structure we can easily double or triple the number of nodes per wavelength. 2D models can reach tens of million of nodes and 3D models must be restricted to a very limited field to be practical. Therefore, parallel computing is an essential paradigm for large-scale models of ultrasound propagation. The current PS parallel implementation is done by solving each equation in (4) on its own processor. We achieve 65% parallel efficiency with this method. For larger problems and additional processors, it is more efficient to parallelize the loops in the FFT and integrator routines and run on a symmetric multiprocessing (SMP) machine. Current implementations indicate SMP efficiencies of around 75% can be achieved on 8 processors.

A bioacoustic modeling example of wavefront aberrations for imaging is shown in Fig. 5. This uses one of the tissue cross-sections from [1] and illustrates both the scale (3 cm x 12 cm) and effectiveness of the PS/R-K method for this class of propagation problem. The five snapshots show the aberrating wavefront as it propagates through the abdominal wall and is absorbed by the PML in the last snapshot, leaving only the complicated diffraction/scattering pattern. The model consists of 1024x4096≈4.2 million grid points. The PS/R-K implementation uses 16 single-precision words per node, so this calculation requires 270 MBytes of RAM. Runtime is 33 hours on an SGI Origin 2000 SMP machine using four processors (achieving 65% parallel efficiency).

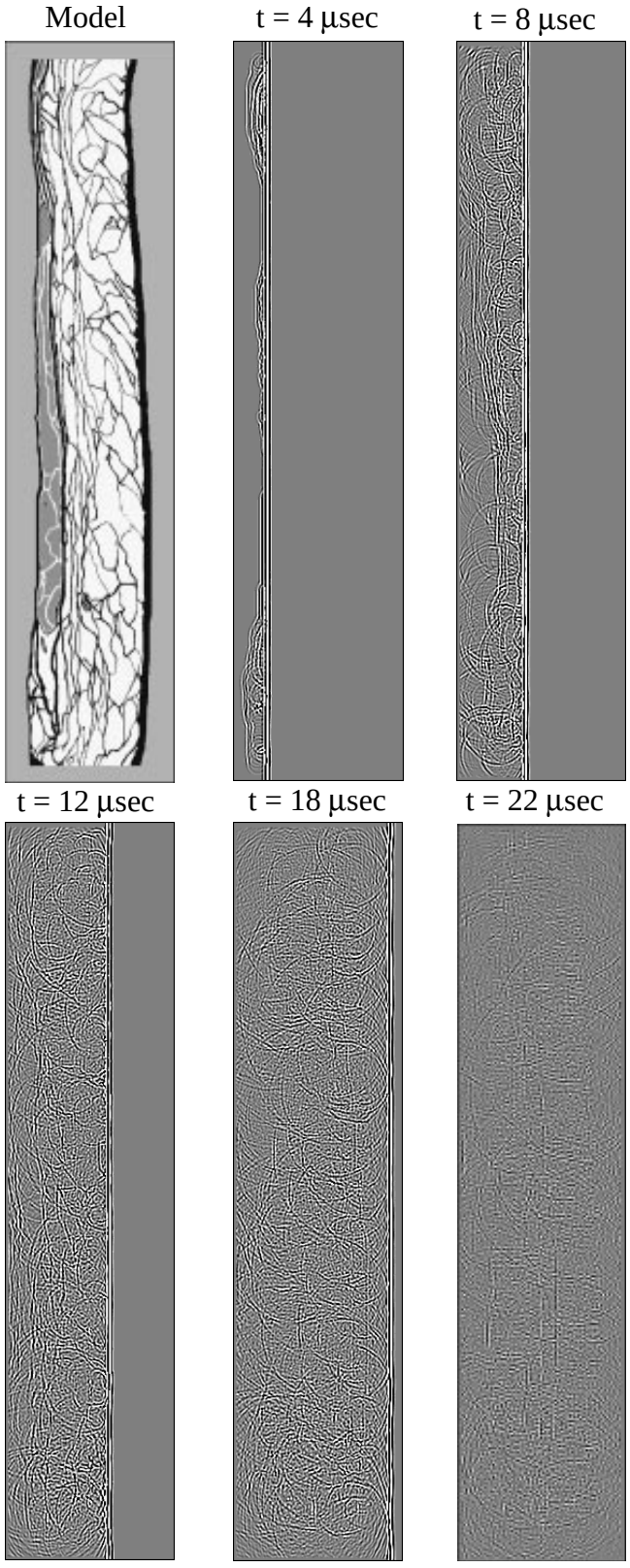

Fig. 5. Large-scale PS calculation of a 2.5 MHz plane wavelet propagating through a 2.1 cm x 11 cm abdominal wall cross-section [1]. Model shown in upper left.

Attenuation and Nonlinearity

Wave attenuation is an essential part of bioacoustic models. There are various attenuation mechanisms including shear and bulk viscosities, a multiplicity of relaxation phenomena, and wave scattering. Since few of these mechanisms can be isolated, aggregate attenuation is measured and characterized by a power law in frequency f as $\alpha=af^b$. For example, in water $a\approx0.0022$ dB/cm/MHz^b, b=2.0, and in muscle tissue $a\approx0.7$ dB/cm/MHz^b, $b\approx1.1$ [11]. Theories and implementations are available, e.g., [12-15], and range from computationally simple stiffness and mass proportional damping to viscoelasticity and related dispersion formulations familiar from classical electromagnetic theory for lossy dielectrics. Note that stiffness proportional damping is ideal in water. For the PS method, Carcione, et al [12] implement an appropriate viscoelastic-dispersive model of relaxation phenomena.

Harmonic distortion due to weak shock effects can also be a fundamental aspect of bioacoustic models. This is included by solving the nonlinear wave equation, which follows by generalizing the constitutive relation in (1) to

$$p = -K\left(\nabla\cdot u + \frac{1}{2}\frac{B}{A}(\nabla\cdot u)^2\right) - (\mu' + \frac{4}{3}\mu)\nabla\cdot v \qquad (5)$$

where stiffness proportional damping is added as a necessary complement (μ is viscosity and μ' is bulk viscosity).

Conclusions

Combining the pseudospectral (PS) method for wave solutions with the perfectly matched layer (PML) makes a formidable algorithm for large-scale ultrasound models in weakly scattering tissue. The PML is very accurate, does not cause any numerical difficulties, and the computational overhead is minor. Further reduction in problem size is offered by wave initialization on a line rather than over the doman. More attention needs to be put on the explicit integration routines used by the PS solver, with respect to stability, accuracy, computational efficiency, and parallelization. Generalizing to the nonlinear wave equation (parameter of nonlinearity, B/A) is straightforward and the PS method's accuracy will extend the number of harmonics significantly before ringing occurs. Attenuation and dispersion models need to be included, but there are precedents and no fundamental limitations are foreseen.

In general, the periodic pseudospectral method combined with Berenger's perfectly matched layer provide a significant advance in the scale and accuracy of bioacoustic models. Wave solvers implementing this algorithm should be useful to ultrasound imaging system researchers and designers as a complement to experiments with phantoms. The algorithm's accuracy and efficiency finally offer a practical numerical model for tissue aberration analysis and the study of deaberration schemes at realistic scales.

Acknowledgements

This work was sponsored by the Defense Advanced Research Projects Agency and the Office of Naval Research, and monitored by Dr. Wallace A. Smith. We extend our appreciation to all involved.

References

[1] L. Hinkelman, T. Mast, M. Orr, V. Sparrow, R. Waag, "Simulation of ultrasonic pulse propagation through the abdominal wall," submitted to *J. Acoust. Soc. Am.*, 1996.

[2] G. Wojcik, J. Mould, F. Lizzi, N. Abboud, M. Ostromogilsky, D. Vaughan, "Nonlinear modeling of therapeutic ultrasound," *Proc. IEEE Ultrasonic Symp*., 1617-1622, 1995.

[3] N. Bojarski, "k-space formulation of the acoustic scattering problem," *Proc. Acoust. Soc. Am. Symp*., 102, 1972.

[4] N. Bojarski, "The k-space formulation of the scattering problem in the time domain: An improved single propagator formulation," *J. Acoust. Soc. Am.*, vol. 77, 3, 826-831, 1985.

[5] O. Kreiss and J. Oliger, "Comparison of accurate methods for the integration of hyperbolic equations," *Tellus*, vol. 24, 199-215, 1972.

[6] B. Fornberg, A Practical Guide to Pseudospectral Methods, Cambridge University Press, 1996.

[7] D. Liu and R. Waag, "Solving the forward scattering problem by the k-space method," Report Draft, Dept. of Electrical Engineering, University of Rochester, Feb. 1997.

[8] R. Kosloff and D. Kosloff, "Absorbing boundaries for wave propagation problems," *J. Comput. Phys.*, vol. 63, 363-376, 1986.

[9] J.-P. Berenger, "A perfectly matched layer for the absorption of electromagnetic waves," *J. Computational Physics*, vol. 114, 185-200, 1994.

[10] X. Yuan, D. Borup, J. Wiskin, M. Berggren, R. Eidens, S. Johnson, "Formulation and validation of Berenger's PML absorbing boundary for the FDTD simulation of acoustic scattering," *IEEE Trans. Ultrason., Ferroelect. and Freq. Control*, vol. 44, **4**, 816-822, 1997.

[11] F. Duck, Phys. Prop. of Tissue, Academic Press, 1990.

[12] J.M. Carcione, D. Kosloff, R. Kosloff, "Viscoelastic wave propagation simulation in the earth," Geophysics, vol. 53, **6**, 769-777, 1988.

[13] A. Nachman, J. Smith, R. Waag, An equation for acoustic propagation in inhomogeneous media with relaxation losses," *J. Acoust. Soc. Am., vol.* 88, **3**, 1584-1595, 1990.

[14] T.L. Szabo, "Time domain wave equations for lossy media obeying a frequency power law," *J. Acoust. Soc. Am., vol.* 96, **1**, 491-500, 1994.

[15] X. Yuan, D. Borup, M. Berggeren, J. Wiskin, S. Johnson, "Simulation of acoustic wave propagation in dispersive media with relaxation losses by using FDTD method with PML absorbing boundary condition," submitted to *IEEE Trans. Ultrason., Ferroelect. and Freq. Control, 1996.*